MADRID
inter.noise 2019
June 16 - 19
NOISE CONTROL FOR A BETTER ENVIRONMENT

Broadband Vibration Isolation for Torsional Rod Using Periodic Structure Theory

Prasad, Rajan[1]
IIT MADRAS
chennai 600036, India

Sarkar, Abhijit[2]
IIT MADRAS
chennai 600036, India

ABSTRACT

For narrow band vibration control applications, the alternating stop band characteristics of periodic structures have been widely used. The objective of the present work is to extend this idea for broadband excitations. We seek to synthesize a torsional periodic structure having the largest fraction of the frequencies falling in the attenuation bands of the structure. The unit cell of such a periodic structure is comprised of two distinct regions having different inertial and stiffness properties. Guidelines are derived for suitable selection of inertial and stiffness properties of the two regions in the unit cell, such that the maximal frequency region corresponds to attenuation bands of the periodic structure. It is found that higher the impedance mismatch between the neighbouring regions of the unit cell leads to maximal attenuating frequencies. It is found that more than 98% of the frequencies are blocked in the extreme case. For torsional excitations, it is shown that large, finite periodic structures corresponding to the optimal unit cell derived using the infinite periodic structure theory has significant vibration isolation benefits in comparison to a homogeneous structure or an arbitrarily chosen periodic structure. The periodic structure synthesized has potential applications in marine engines, where long rods are required for power transmission.

Keywords: Periodic structure, band gap, torsional rod
I-INCE Classification of Subject Number: 30
(see http://i-ince.org/files/data/classification.pdf)

[1]rajnitdgp2007@gmail.com
[2]asarkar@iitm.ac.in

1. INTRODUCTION

A periodic structure consist of a repeating unit, defined as a unit cell. The wave propagation in the periodic structure comprises of well-defined frequency ranges wherein the amplitude of the wave attenuates exponentially. These frequency bands are defined as the stop band of the periodic structure. The frequency bands other than stop bands are termed as pass-band where the waves are transmitted without any attenuation. The remarkable characteristics of a periodic structure are the presence of the stop band and pass-band over the frequency domain. The pass-band and stop-band for such structures depend upon the unit cell. The attenuation characteristics of the periodic structure for the frequency range within the stop band are particularly significant in noise and vibration control applications. The pass-band and stop band characteristics for rods [1],beams [2] and plates [3] have been studied theoretically and experimentally.

Torsional vibration is one of the common modes of vibration in long shafts. The long shafts are typically used in power transmission in naval engines. The unbalanced forces leads to the torsional vibration for the shafts. As a result the service life of the shaft and its reliability gets affected. Various studies have investigated the band gap properties of periodic rod undergoing torsional mode of vibration. Torsional waves propagation in rod having stepped diameter has been studied in [4, 5]. The periodic torsional rod is used in detecting torsional waves with the help of transducer in [6]. Low frequency torsional band gaps in shafts were studied by Dianlong et.al and the effect of shaft material was investigated. [7]. The band structure of periodic shafts with various attached structure were studied by Yubao et.al [8]. In all the works stated above the shaft is designed for a narrow band excitation. In these narrow band excitation the vibration remain localized and are not transmitted away from the source. Thus an important goal would be to design structure for broadband excitation. The objective of these work is to design a bi-material periodic torsional rod consisting of two different regions with two different regions refer Fig.1. The design objective is attain attenuation across all the frequency ranges. The aim is to evaluate the optimal combination of (viz..,G_1J_1/G_2J_2, ρ_1J_1/ρ_2J_2) between the adjacent region which will give rise to maximal attenuation characteristics across the frequency spectrum.

2. TORSIONAL WAVES IN AN INFINITE BIMATERIAL ROD

Consider a periodically segmented rod of infinite length as shown in Fig. 1 undergoing torsional motion. The unit cell is made up of two different constituents and different geometric properties which is captured by the function $\alpha(x) = G(x)J(x)$ and $\Phi(x) = \rho(x)J(x)$ as torsional stiffness and polar mass moment of inertia. The governing equation of the structure is [9]

$$\frac{\partial}{\partial x}\left(\alpha(x)\frac{\partial}{\partial x}\theta(x,t)\right) = \Phi(x)\frac{\partial^2}{\partial t^2}\theta(x,t) \tag{1}$$

We consider a harmonic solution of the form $\theta = \Theta(x)e^{i\omega t}$. Thus, the above equation becomes,

$$\frac{\mathrm{d}}{\mathrm{d}x}\left(\alpha(x)\frac{\mathrm{d}\Theta}{\mathrm{d}x}\right) - \Phi(x)\omega^2\Theta(x) = 0 \tag{2}$$

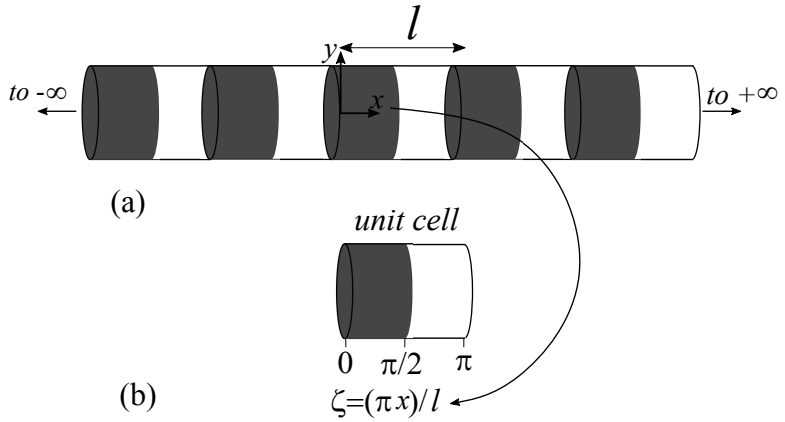

Figure 1: (a) Infinite one-dimensional periodic structure (b) Unit cell along the the non-dimensional coordinate ζ.

2.2.1. Transfer Matrix formulation

The function $\alpha(x)$ and $\Phi(x)$ are periodic in x with a periodicity of l. $\alpha(x)$ is given by

$$\alpha(x) = \begin{cases} (\frac{G_1J_1+G_2J_2}{2}) + (\frac{G_1J_1-G_2J_2}{2}) = \alpha_a + \frac{\alpha_f}{2} & 0 \le x \le \frac{l}{2} \\ (\frac{G_1J_1+G_2J_2}{2}) - (\frac{G_1J_1-G_2J_2}{2}) = \alpha_a - \frac{\alpha_f}{2} & \frac{l}{2} \le x \le l \end{cases} \tag{3}$$

α_a thus represents the average value of the property, Similarly α_f represents the fluctuating value of the property. Along similar lines, for $\Phi(x)$ we have

$$\Phi(x) = \begin{cases} (\frac{\rho_1J_1+\rho_2J_2}{2}) + (\frac{\rho_1J_1-\rho_2J_2}{2}) = \Phi_a + \frac{\Phi_f}{2} & 0 \le x \le \frac{l}{2} \\ (\frac{\rho_1J_1+\rho_2J_2}{2}) - (\frac{\rho_1J_1-\rho_2J_2}{2}) = \Phi_a - \frac{\Phi_f}{2} & \frac{l}{2} \le x \le l \end{cases} \tag{4}$$

Equation (2) can thus be written as :

$$\begin{aligned} (\alpha_a + \frac{1}{2}\alpha_f)\frac{\mathrm{d}^2\Theta}{\mathrm{d}x^2} + (\Phi_a + \frac{1}{2}\Phi_f)\Theta(x)\omega^2 = 0 \quad \text{for } 0 \le x \le \frac{l}{2} \\ (\alpha_a - \frac{1}{2}\alpha_f)\frac{\mathrm{d}^2\Theta}{\mathrm{d}x^2} + (\Phi_a - \frac{1}{2}\Phi_f)\Theta(x)\omega^2 = 0 \quad \text{for } \frac{l}{2} \le x \le l \end{aligned} \tag{5}$$

Next, we introduce a non-dimensional variable $\zeta = \frac{\pi x}{l}$, Note the functions Φ and α are periodic with a periodicity of π in ζ. Eq. (5) is thus non-dimensionalized to the following

$$\frac{\mathrm{d}^2\Theta}{\mathrm{d}\zeta^2} + {}_1{}^2\Theta(\zeta) = 0 \quad \text{for } 0 \le \zeta \le \frac{\pi}{2} \tag{6a}$$

$$\frac{\mathrm{d}^2\Theta}{\mathrm{d}\zeta^2} + {}_2{}^2\Theta(\zeta) = 0 \quad \text{for } \frac{\pi}{2} \le \zeta \le \pi \tag{6b}$$

where,

$$\begin{aligned} \beta_1{}^2 = \frac{\delta+\epsilon}{1+\frac{1}{2}\gamma} \ , \beta_2{}^2 = \frac{\delta-\epsilon}{1-\frac{1}{2}\gamma} \ , \\ \delta = \frac{\Phi_a l^2\omega^2}{\pi^2\alpha_a} \ , \epsilon = \frac{\Phi_f l^2\omega^2}{\pi^2\alpha_a} \ , \gamma = \frac{\alpha_f}{\alpha_a} \end{aligned} \tag{7}$$

2.1.1 Transfer matrix Derivation

We seek solution of Eq. (6a) and Eq. (6b) as the superposition of two waves namely :- (1) travelling along $+\zeta$ (2) travelling along $-\zeta$

$$\Theta(\zeta) = \begin{cases} A_1 e^{i_1\zeta} + A_2 e^{-i_1\zeta} & \text{for } 0 \le \zeta \le \frac{\pi}{2} \\ B_1 e^{i_2\zeta} + B_2 e^{-i_2\zeta} & \text{for } \frac{\pi}{2} \le \zeta \le \pi \end{cases} \tag{8}$$

Considering the unit cell in Fig. 1. The twisting moment $M^*(\zeta)$ is non-dimensionalized with respect to parameter α_a along ζ-direction in the region $\{1\}$ as:

$$M^*(\zeta) = (1 + \frac{1}{2}\gamma)\frac{d\Theta}{d\zeta} \tag{9}$$

In the transfer matrix method, state vectors at $\zeta = \frac{n\pi}{2}$, $n = 0, 1, 2, \ldots$ are defined. The state vector $\phi(\zeta)$ comprises the non-dimensional angular displacement $\Theta(\zeta)$ and the non-dimensional twisting moment $M^*(\zeta)$ in the ζ-direction. The transfer matrix establishes a relation between state vectors at $\zeta = \frac{n\pi}{2}$ and state vectors at $\zeta = \frac{(n+1)\pi}{2}$. In the following, the transfer matrix relating the state vectors at $\zeta = 0$ and $\zeta = \frac{\pi}{2}$ is derived. To derive the expressions of the transfer matrix element, angular displacement and moment are written in the matrix form as $\zeta \to 0$ from the right. Using Eq. 8 and Eq. 9, we have

$$\begin{aligned} \{\phi(0^+)\} &= \begin{Bmatrix} \Theta(0^+) \\ M^*(0^+) \end{Bmatrix} = \begin{bmatrix} 1 & 1 \\ i_1(1 + \frac{1}{2}\gamma) & -i_1(1 + \frac{1}{2}\gamma) \end{bmatrix} \begin{Bmatrix} A_1 \\ A_2 \end{Bmatrix} \\ &= [C] \begin{Bmatrix} A_1 \\ A_2 \end{Bmatrix} \end{aligned} \tag{10}$$

Similarly,
$$\{\phi(\frac{\pi^-}{2})\} = \begin{Bmatrix} \Theta(\frac{\pi}{2}^-) \\ M^*(\frac{\pi}{2}^-) \end{Bmatrix} = [C] \begin{bmatrix} e^{i_1\frac{\pi}{2}^-} & 0 \\ 0 & e^{-i_1\frac{\pi}{2}^-} \end{bmatrix} \begin{Bmatrix} A_1 \\ A_2 \end{Bmatrix} \tag{11}$$

Using Eq. (10) in Eq. (11), we get

$$\begin{aligned} \begin{Bmatrix} \Theta(\frac{\pi}{2}^-) \\ M^*(\frac{\pi}{2}^-) \end{Bmatrix} &= [C][P][C]^{-1} \begin{Bmatrix} U(0^+) \\ f^*(0^+) \end{Bmatrix} \\ &= [T_1] \begin{Bmatrix} U(0^+) \\ f^*(0^+) \end{Bmatrix} \end{aligned} \tag{12}$$

Here $T_1 = CPC^{-1}$ is the transfer matrix relating the state vectors between the left end and the right end of the region $0 < \zeta < \frac{\pi}{2}$. Similarly T_2 is obtained for the region $\frac{\pi}{2} < \zeta < \pi$. Thus, we have

$$\{\phi(\frac{\pi^-}{2})\} = [T_1]\{\phi(0^+)\} \ , \ \{\phi(\pi^-)\} = [T_2]\{\phi(\frac{\pi^+}{2})\}$$

Employing the continuity condition at $\zeta = \frac{\pi}{2}$, we have $\phi(\frac{\pi}{2}^+) = \phi(\frac{\pi}{2}^-)$. Thus, the state vectors at $\zeta = 0^+$ and $\zeta = \pi^-$ are related through the following transfer matrix :

$$\begin{aligned} \{\phi(\pi^-)\} &= [T_2]\{\phi(\frac{\pi^+}{2})\} = [T_2]\{\phi(\frac{\pi^-}{2})\} \\ &= [T_2][T_1]\{\phi(0^+)\} = [T(\delta, \epsilon, \gamma)]\{\phi(0^+)\} \end{aligned} \tag{13}$$

Note, the transfer matrix T relating the state vectors of the unit cell is dependent on δ, ϵ and γ. According to Floquet-Bloch theorem [10],

$$\{\phi(\zeta + \pi)\} = e^{\mu}\{\phi(\zeta)\} \Rightarrow \{\phi(\pi^+)\} = e^{\mu}\{\phi(0^+)\} \tag{14}$$

Using Eq. (14) and Eq. (13) the following eigenvalue problem is formulated as $[T(\delta, \epsilon, \gamma) - I\lambda]\{\phi(0^+)\} = 0$, where, $\lambda = e^{\mu}$ and μ is the propagation constant.

3. EIGENVALUE MAP

The transfer matrix T derived in section 2.1.1 is a symplectic matrix [11]. As a result of that the two eigenvalues of T occur in pair as λ and $\frac{1}{\lambda}$. These eigenvalues can be determined for the given value of the parameters, δ, ϵ, and γ . As studied by mead [12], there are two possibilities for the eigenvalues :- (a) the eigenvalue pair is a set of complex conjugates lying on the unit circle (b) the eigenvalue pair is real with one lying inside and the other lying outside the unit circle. These are schematically illustrated in Fig. 2. the attenuation band and pass-band characteristics can be determined that are associated with each of these cases, If the eigenvalues lie on the unit circle of the complex plane *viz.*$|\lambda| = 1$, then the corresponding parameters lie within a pass-band region. The real eigenvalues correspond to the stop band region. For a given a material combination γ is fixed, with δ and ϵ turning out to be frequency dependent parameter. The frequency associated with either a propagation band band or an attenuation band cab be identified using δ and ϵ. Thus for a given γ we construct an eigenvalue map for the transfer matrix for a range of δ-ϵ values. The eigenvalue which lies in the pass band region are shown in grey and the complimentary region is shown in white. Using this convention the eigenvalue map is generated for different case in the subsequent section. More details can be found in [13]

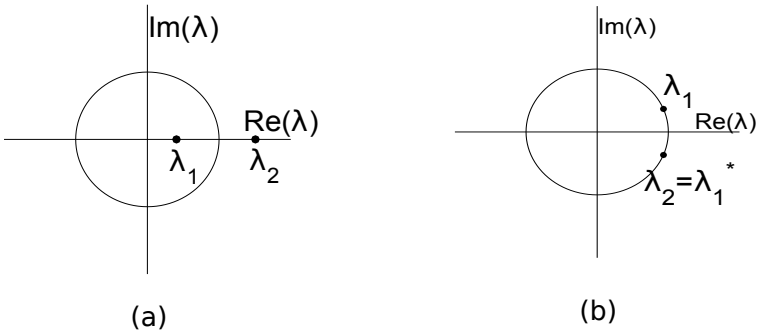

Figure 2: Eigenvalues of the transfer matrix of the periodic torsional rod (a) conjugate pair lying on the unit circle in the complex plane (b) & (c) lying on the real axis.

3.3.1. Effects of variation in inertial properties of the unit cell

The eigenvalue map for $\gamma = 0$ is presented which stands for same torsional stiffnes on either side of the unit cell Fig. 1. From Eq. (7), we have

$$\frac{\epsilon}{\delta} = \frac{\Phi_f}{\Phi_a} = \xi \tag{15}$$

As per Eq. 7, δ and ϵ are both function of ω . The locus of $\epsilon - \delta$ points in the parameter space is a straight line. These lines are defined as ω-lines for the subsequent discussion. Using the method as described in section 3, for $\gamma = 0$, we evaluate the eigenvalues of the transfer matrix T for the different values of ϵ and δ. The regions of ϵ and δ parameter space are shown in grey for which the eigenvalues lie on the unit circle. These parameter space is identified as propagating zone whereas the complimentary zone is identified as attenuation zone. The ω-lines given by Eq. 7 alternatively intersect the propagation and attenuation zones. The frequency bands are evaluated by noting the intersection points

Table 1: Co-ordinates-of the intersection points of the eigenvalue map in Fig. 3 with the ω-line corresponds to $\epsilon/\delta = 1$

Points	δ	ϵ	Ω
a	.747	.747	2.71
b	1.42	1.42	3.74
c	3.78	3.78	6.10
d	4.88	4.88	6.94

of the line with white regions and is shown in Table 1. The associated non-dimensional frequency can be evaluated as

$$\omega = \sqrt{\frac{\delta\pi^2\alpha_a}{\Phi_a l^2}} \Rightarrow \Omega = \frac{\omega l}{\sqrt{\frac{\alpha_a}{\phi_a}}} = \pi\sqrt{\delta} \tag{16}$$

From eigenvalue map of Fig 3, it is easy to see that increase slope of ω line is favourable

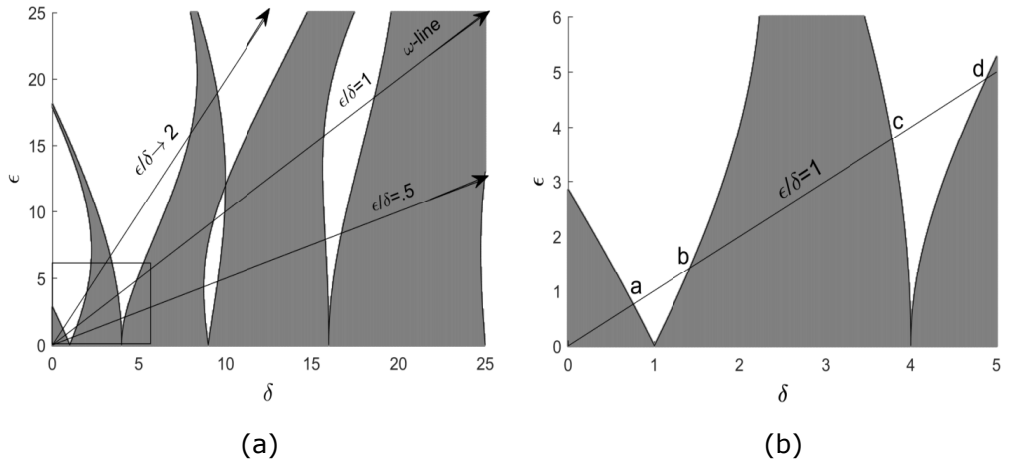

Figure 3: (a) Eigenvalue map of a bi-material unit torsional rod with identical stiffness between adjacent regions ($\gamma = 0$) (b) Enlarged view of the same for mass moment of inertia ratio $\frac{\epsilon}{\delta} = 1$. The white and grey region in the $\epsilon - \delta$ parameter space represents stop band and pass band characteristics, respectively.

for having maximal frequency in the attenuation region. Henceforth the values of $(\frac{\Phi_f}{\Phi_a})$ can be chosen to be maximum. However for the mass function $\Phi(x) > 0$ within the unit cell, the slope needs to satisfy the condition $\frac{\Phi_f}{\Phi_a} < 2$. The limiting value of $\frac{\Phi_f}{\Phi_a} \to 2^-$ results in best attenuation characteristics of the structure. The non-dimensional frequency of first four band gap is presented in Table 2

3.3.2. Change of stiffness and inertia

In this section the effect of simultaneous variation of stiffness and inertial properties within the unit cell is investigated. Similar to the analysis in section 3.3.1 the eigenvalue map for different values of γ over the $\epsilon - \delta$ parameter space is developed. The range of γ chosen is such that the stiffness function $\alpha(x) > 0$ within the unit cell. This condition

Table 2: Non-dimensional frequencies corresponding to the stop-bands for bi material periodic torsional rod with optimal mass moment of inertia ratio $\xi = 2^-$ and uniform stiffness $\gamma = 0$.

1st Band	2nd Band	3rd Band	4th Band	% Stop Band
2.443-4.443	5.739-8.891	9.696-13.348	13.910-17.818	71.31

Table 3: Non-dimensional frequencies for the stop band of a bi-material rod for optimal choice of mass moment of inertia ratio ($\xi = 2^-$) and stiffness ratio ($\gamma = 2^-$). The results are obtained using eigenvalue map (EVM) & Finite element method (FEM).

Methods	1st Band	2nd Band	3rd Band	4th Band
EVM	.002-6.26	6.30-12.54	12.58-18.83	18.87-25.12
FEM	.002-6.26	6.30-12.54	12.58-18.83	18.87-25.12

implies that $0 < \gamma < 2$ refer Eq. 3. The eigenvalue map for $\gamma = .5, 1, 1.5, 1.9$ is shown in Fig 4. As shown earlier in section 3.3.1 that optimal ω lines has a slope of 2^-. These optimal ω lines are also overlaid in Fig. 4. It is observed from the figure that with increase in γ the attenuation frequency bands widens. The widest frequency bands are viewed at $\xi, \gamma \to 2^-$. Physically it implies that the inertial and stiffness characteristics of one region of the unit cell is extremely high in comparison to other region.

3.3.3. Validation

The optimal unit cell synthesized in the previous section having the widest frequency bands over the entire frequency range is considered. The band gap result of optimal unit cell at $\xi, \gamma \to 2^-$is shown in Table 3. It is seen that 99 % of the frequency range falls withing the attenuation region. The frequency bands can also be calculated using an FEM- based method (as given in [14]). These result is also shown along side for the optimal unit cell. It is noted that both the approaches are in excellent co-relation.

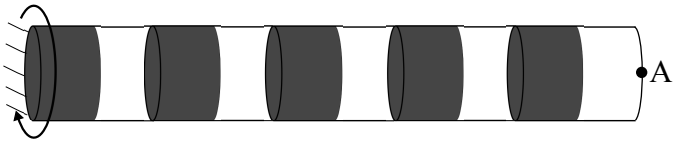

Figure 5: Finite bi-material periodic rod .

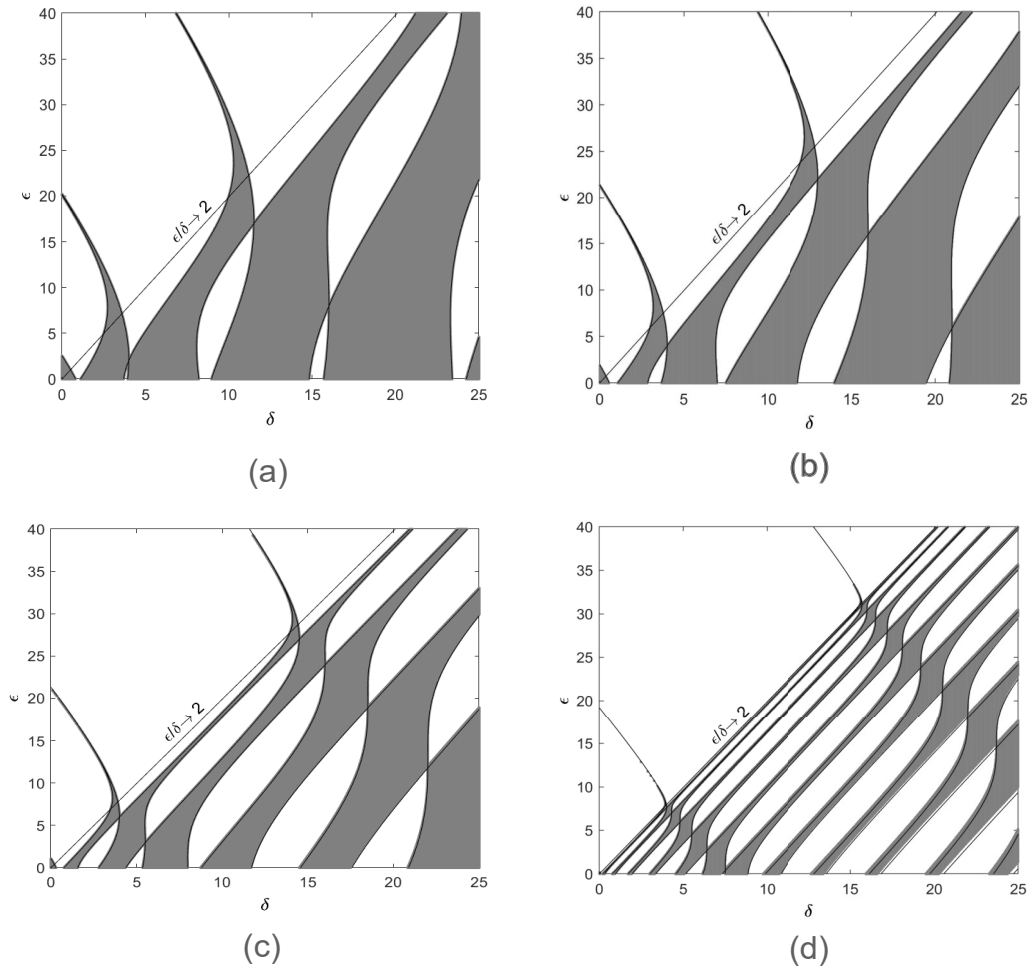

Figure 4: Eigenvalue map of a bi-material periodic torsional rod for mass moment inertia ratio $\xi \to 2^-$ and different values of of stiffness ratio (γ). The white and the grey region in the $\epsilon-\delta$ parameter space represents stop band and pass band characteristics, respectively.

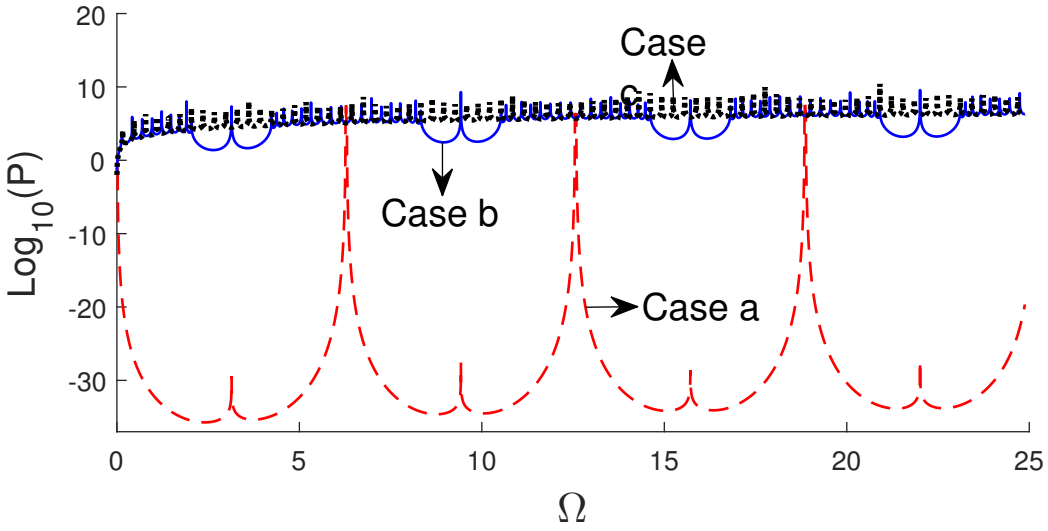

Figure 6: Tip Response at A due to a harmonic base angular acceleration for (a) optimal stiffness and mass ratio $\xi, \gamma \to 2^-$ (b) sub-optimal ratio $\xi, \gamma = 1$ and (c) homogenous material $\xi, \gamma = 0$.

3.3.4. Finite Periodic torsional Rod structure response

A finite periodic structure comprising of ten periodic unit cell exhibit similar qualitative result as that of infinite periodic structure. For the purpose of demonstration about ten periodic unit is considered 5. Three cases are considered, namely (a) the unit cell with $\xi, \gamma \rightarrow 2^{-}$ (b) the unit cell with $\xi, \gamma = 1$ (c) the unit cell with $\xi, \gamma = 0$, which correspond to the homogeneous structure. The structure is subjected to harmonic angular acceleration at the base. For the simulation of structure response the commercial software ANSYS is used. The absolute angular displacement P(Ω) at the tip of the structure is calculated for a range of frequencies and is shown in Fig. 6. The FRF shows that the periodic structure designed using optimal unit cell, has very favourable attenuation characteristics for all frequency ranges. Hence it has practical utility in designing structure susceptible to broadband excitation.

4. CONCLUSIONS

In conclusion, it is shown that eigenvalue map (EVM) is very effective in arriving at the optimal ratio of stiffness and mass to get maximal attenuation across frequency range. It is also shown that optimal unit cell periodic structure induces maximal attenuation band gap than any other homogeneous structure. The torsional band gap achieved can be effectively be used in controlling broadband vibration in long shafts typically used in turbines and marine engine. From design point of view, it is desirable to have the stiffness and mass of one region of the unit cell to be much higher than the other region to achieve broadband isolation. The optimal combination of mass moment of inertia and torsional stiffness ratio can only be achieved in a limiting sense by appropriate choice of both material and geometric parameter.

5. REFERENCES

[1] Mahmoud I Hussein, Gregory M Hulbert, and Richard A Scott. Dispersive elastodynamics of 1d banded materials and structures: analysis. *Journal of sound and vibration*, 289(4):779–806, 2006.

[2] Denys J Mead. Free wave propagation in periodically supported, infinite beams. *Journal of Sound and Vibration*, 11(2):181–197, 1970.

[3] Denys J Mead. A new method of analyzing wave propagation in periodic structures; applications to periodic timoshenko beams and stiffened plates. *Journal of Sound and Vibration*, 104(1):9–27, 1986.

[4] Helge E Engan. Torsional wave scattering from a diameter step in a rod. *The Journal of the Acoustical Society of America*, 104(4):2015–2024, 1998.

[5] K Liu, S Xie, and H Sun. Reflection characteristics of torsional waves in transversely isotropic stepped bars. *Computer methods in applied mechanics and engineering*, 153(1-2):107–115, 1998.

[6] A Morales, J Flores, L Gutiérrez, and RA Méndez-Sánchez. Compressional and torsional wave amplitudes in rods with periodic structures. *The Journal of the Acoustical Society of America*, 112(5):1961–1967, 2002.

[7] Dianlong Yu, Yaozong Liu, Gang Wang, Li Cai, and Jing Qiu. Low frequency torsional vibration gaps in the shaft with locally resonant structures. *Physics Letters A*, 348(3-6):410–415, 2006.

[8] Yubao Song, Jihong Wen, Dianlong Yu, and Xisen Wen. Analysis and enhancement of torsional vibration stopbands in a periodic shaft system. *Journal Of Physics D: Applied Physics*, 46(14):145306, 2013.

[9] Leonard Meirovitch. *Elements of vibration analysis*. McGraw-Hill Companies, 1975.

[10] G. Floquet. On the linear differential equations with periodic coefficients. *Annales scientifiques de l'École Normale Supérieure*, 12:47–88, 1883.

[11] WX Zhong and FW Williams. Wave problems for repetitive structures and symplectic mathematics. *Proceedings of the Institution of Mechanical Engineers, Part C: Journal of Mechanical Engineering Science*, 206(6):371–379, 1992.

[12] Denys J Mead. Wave propagation and natural modes in periodic systems: I. mono-coupled systems. *Journal of Sound and Vibration*, 40(1):1–18, 1975.

[13] Rajan Prasad and Abhijit Sarkar. Broadband vibration isolation for rods and beams using periodic structure theory. *Journal of Applied Mechanics*, 86(2):021004, 2019.

[14] Ruth M Orris and M Petyt. A finite element study of harmonic wave propagation in periodic structures. *Journal of Sound and Vibration*, 33(2):223–236, 1974.